Synthesis of up-conversion fluorescence N-doped carbon dots with high selectivity and sensitivity for detection of Cu^{2+} ions

Yuanyuan Xiong [1], Mengxiao Chen [1], Zhen Mao [1], Yiqing Deng [1], Jing He [1], Huaixuan Mu [1], Peini Li [1], Wangcai Zou [1] and Qiang Zhao [1,*]

[1] School of Chemical Engineering, Sichuan University, No.24 South Section 1, Yihuan Road, Chengdu, 610065, China; E-mail: zhaoqiang@scu.edu.cn

The synthesis of N-CDs-1[1]

In a typical procedure, 10 mM of the citric acids and 2.5 mM niacinamide were filled into 15 ml Teflon inners, respectively. Ultrapure water was added until the mixtures were completely dissolved, and then heated the inners in a 70 °C water bath until the liquid became a viscous solution. Then, the solution was placed into a stainless-steel reactor and reacted at 200 °C for 5 h. The solid products were completely dissolved by adding sodium hydroxide. The solutions were placed into a 1000 Dalton dialysis bag and dialyzed for 3 d. Then, the sample was lyophilized to obtain the c-CDs.

The synthesis of N-CDs-2[2]

Typically, 3.6782 g of l-Glu (0.025 mol) and 0.2703 g of MPD (0.0025 mol) were added to 100 mL of ultrapure water. After 30 min of magnetic stirring, the mixture was transferred to a 250 mL Teflon reactor and allowed to react at 200 °C for 6 h. When the reactor was cooled to room temperature, a solution of CQDs was obtained. Then, the sample was lyophilized to obtain the product.

The detection of metal ions

N-CDs-1: 600 μL of N-CDs-1 solution was added into 9mL ultra-water for dilution and named as A solution. Then 300 μL metal ions solution (0.2 mol/L) was added and ultrasonic for 5min. After that, the PL intensity of mixed solution was measured at 410 nm. Additionally, a series of Fe^{3+} solutions with concentration of 30-1000 μM were prepared and 300 L Fe^{3+} solution was mixed with diluted N-CDs-1 (A solution). After ultrasonic for 5 min, the PL intensity of mixed solution was measured at 410 nm to conduct interference test. Also, the operations of up-conversion PL system were same as above but the excitation wavelength was 808 nm.

N-CDs-2: 200 μg/mL N-CDs-2 solution was mixed with metal ions solution (1 mg/mL) with ratio of 4:1, and then the PL intensity of mixed solution was measured at 380 nm. Additionally, a series of Fe^{3+} solutions with concentration of 25-750 mg/mL was prepared. 200 μL N-CDs-2 solution and 300 μL Fe^{3+} ions solution were added into 2.5 mL ultra-water. And then the PL intensity of mixed solution was measured at 410 nm to study interference test.

Characterizations

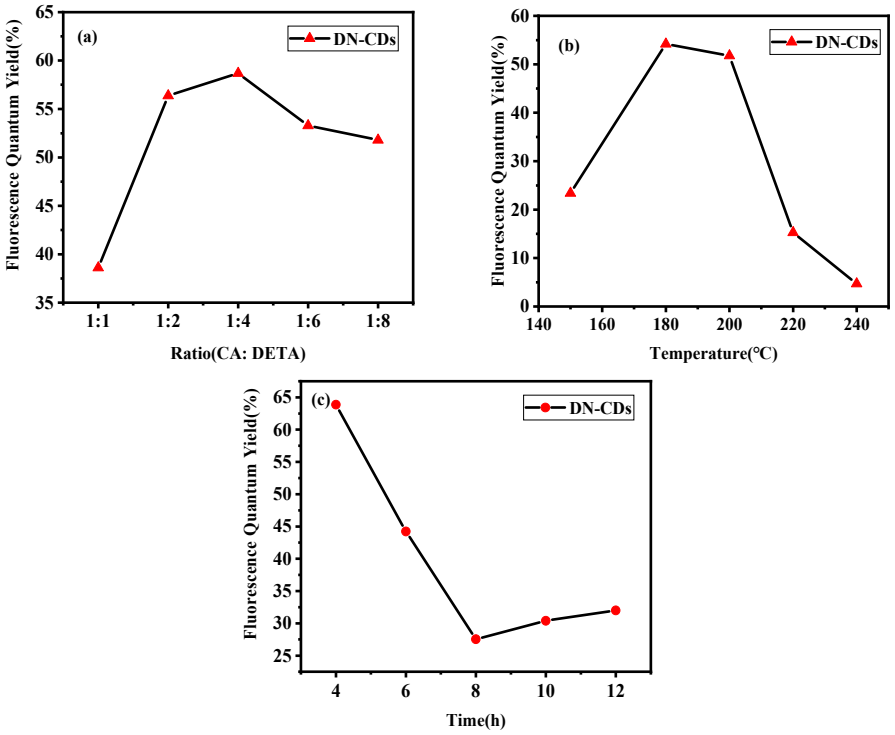

Figure S1. The trends of the quantum yield fluorescence of N-doped carbon dots at different ratio of carbon source and nitrogen source (a), reaction temperature (b), reaction time (c).

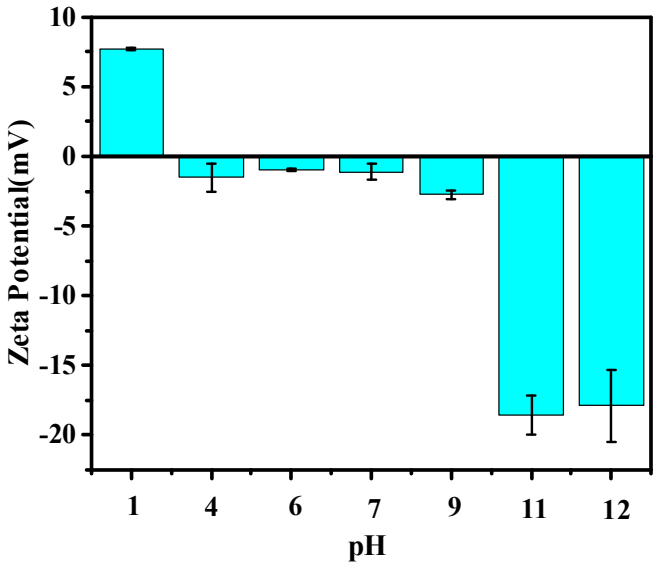

Figure S2. The Zeta potential of DN-CDs under different pH.

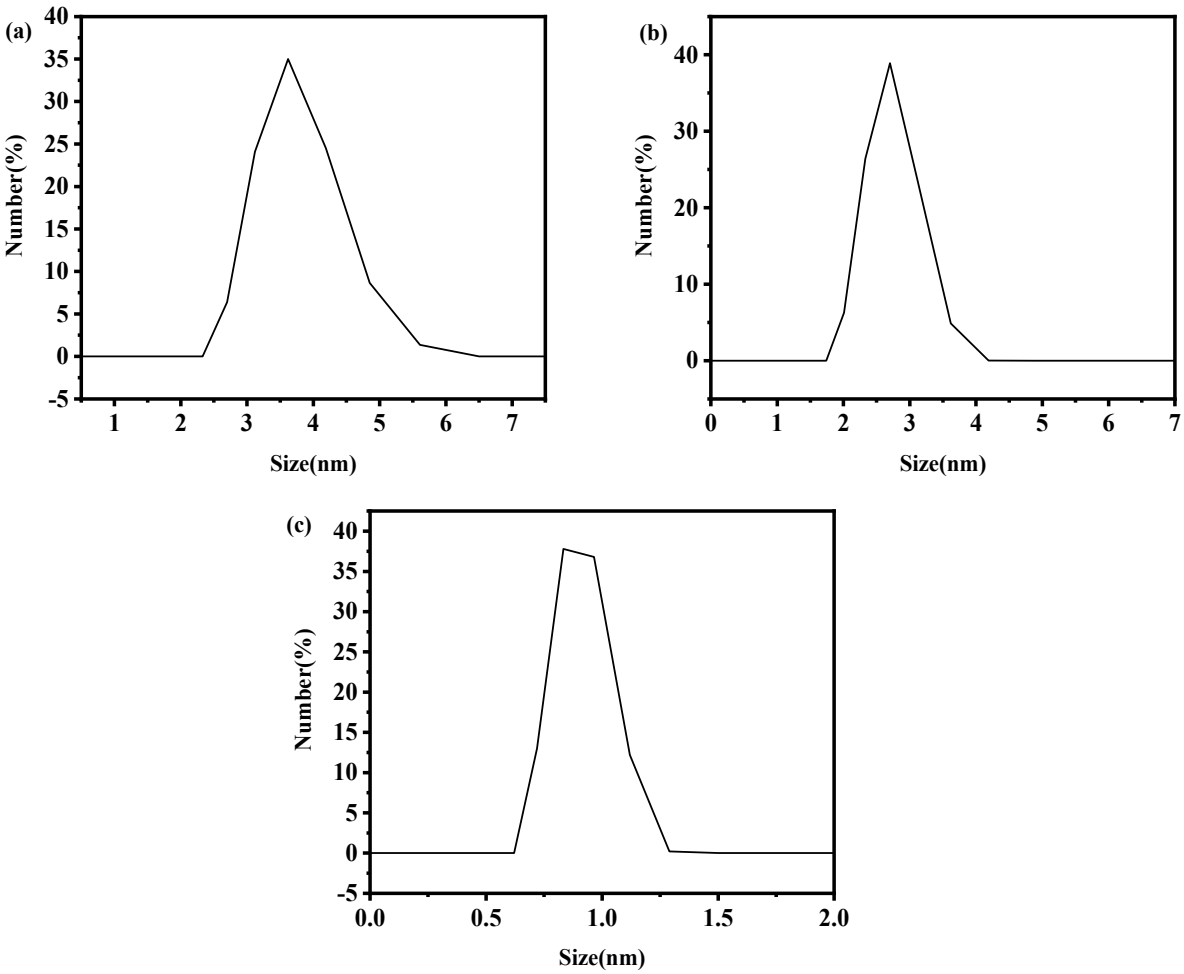

Figure S3. The DLS of DN-CDs in aqueous solution at (a) pH = 1, (b) pH = 7 and (c) pH = 13.

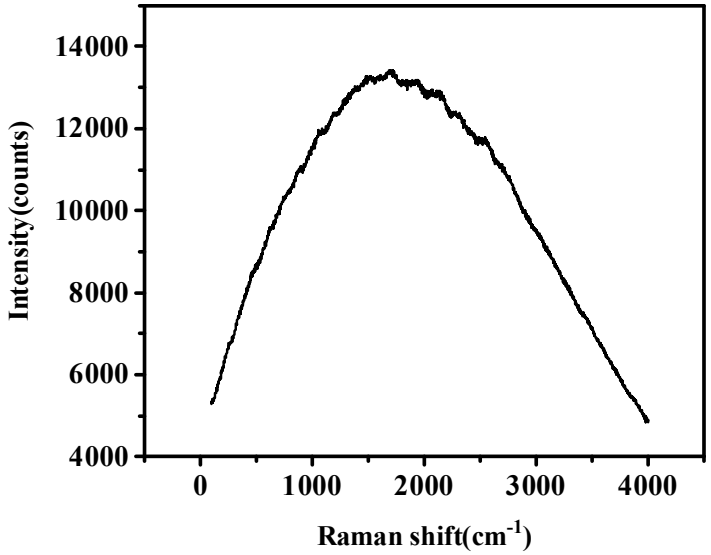

Figure S4. The Raman spectrum of DN-CDs.

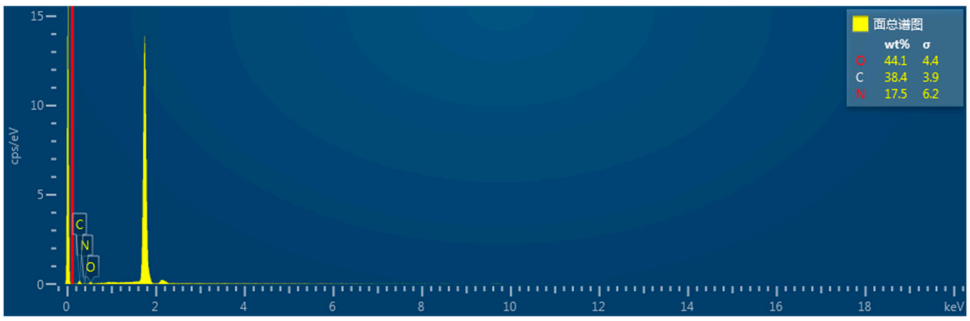

Figure S5. The EDS of DN-CDs.

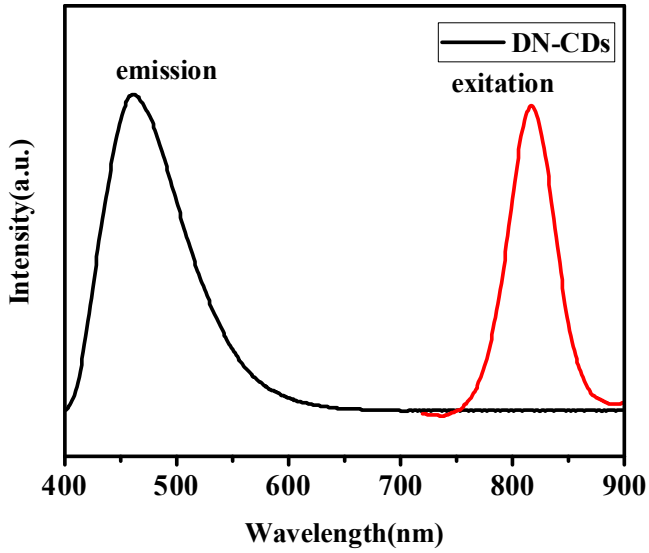

Figure S6. The up-conversion PL spectra of DN-CDs. (The emission spectrum at maximum excitation wavelength at 820 nm and the excitation spectrum at the maximum emission wavelength of 450 nm).

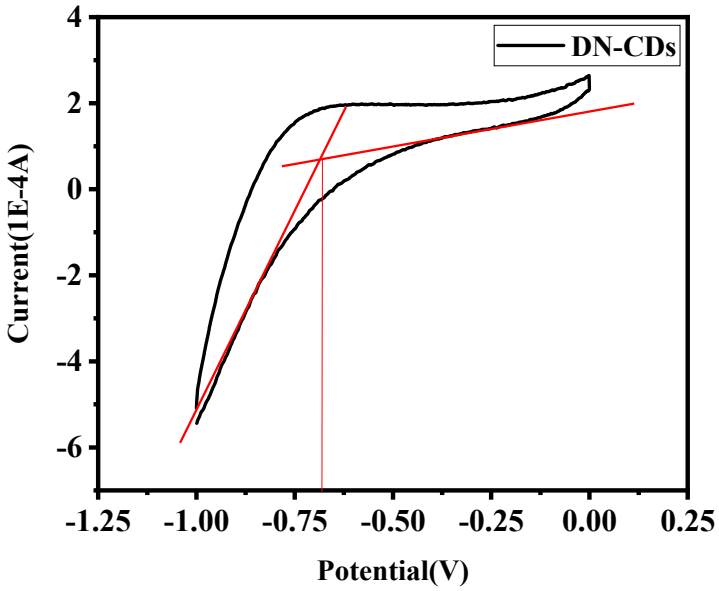

Figure S7. The CV plot of DN-CDs.

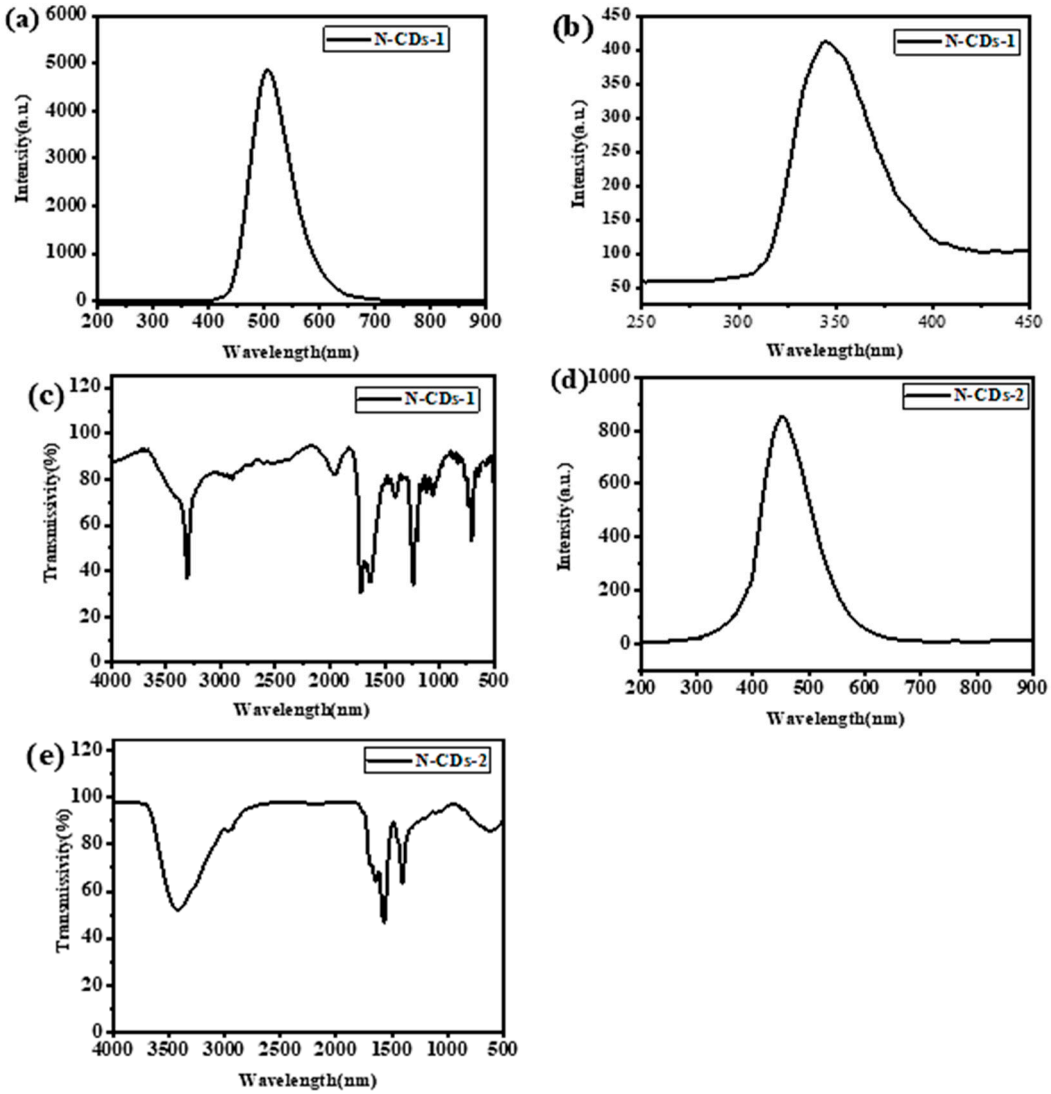

Figure S8. (**a-c**) The fluorescence emission spectra at λex = 450 nm and λex = 600 nm and FT-IR spectra of N-CDs-1; (**d-e**) The fluorescence emission spectra at λex = 380 nm and FT-IR spectra of N-CDs-2.

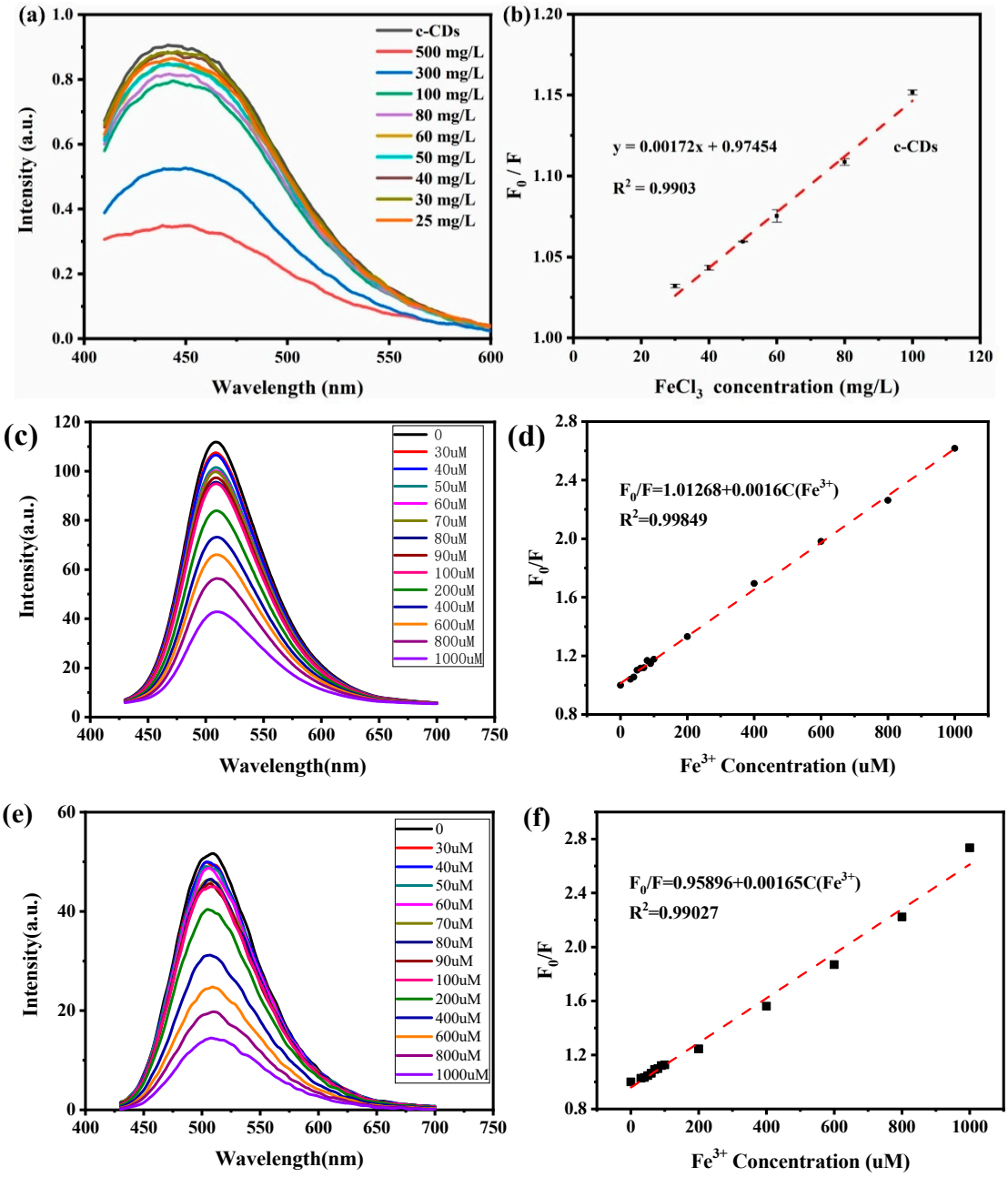

Figure S9. The PL quenching efficiency of (**a**) N-CDs-2 at λex = 380 nm and (**c**) N-CDs-1 at λex = 410 nm and (**e**) at λex = 808 nm at different concentration of Fe^{3+} ions and the linear relationship between PL intensity and Fe^{3+} ions ('F0' is PL intensity in the absence of Fe^{3+} ions and 'F' is in the presence of Fe^{3+} ions) of (**b**) N-CDs-2 at λex = 380 nm, (**d**) N-CDs-1 at λex = 410 nm and (**f**) at λex = 808 nm.

Table. S1 The detection parameters for selective detection of metal ions (Cu^{2+} and Fe^{3+}) with different N-doped carbon dots.

Carbon source	method	Atom ratio(C:O:N)	N/O	QY	Functional group	The detection of metal ions	LOD	Range of detection	Ref.
benzylchloroformate	Hydrothermal method	76.82: 17.95: 3.96	0.22	31.5%	Amine, boronic acid	Fe^{3+}	0.1 μM	1-80 μM	[3]
Porphyromonas gingivalis	hydrothermal method	71.30: 21.53: 6.54	0.30	4.83 %	Hydroxyl, amine	Fe^{3+}	1.85 μM	0-500 μM	[4]
hydroquinone	High-temperature feflux	74.10: 20.7: 5.20	0.25	0.59 %	Hydroxyl, amine	Fe^{3+}	0.86 μM	0-60 μM	[5]
N-methyl-2-pyrrolidone	Hydrothermal method	67.5: 23.3: 9.3	0.40	32.5%	Hydroxyl, amine	Fe^{3+}	59 nM	0-50 uM	[6]
L-cysteine	Hydrothermal method	59.0: 27.2: 6.5	0.24	/	Carboxyl. amine	Fe^{3+}	69 nM	0.3-20 uM	[7]
Waste biomass	Hydrothermal method	63.0: 31.0: 6	0.19	7%	Hydroxyl, carboxyl and amine	Fe^{3+}	1.4 uM	5-25 uM	[8]
hydroquinone	hydrothermal method	60.1: 27.3: 11.0	0.40	19.20 %	Silicon-based	Fe^{3+}	/	0-120 μM	[9]
p-Coumaric acid	hydrothermal method	80.9: 6.4: 12.7	1.98	34.4%	hydroxyl, amine, and carbonyl	Cu^{2+}	10 nM	0-10 uM	[10]
Oil red O	solvothermal method	76.1: 10.1: 13.8	1.37	68%	Amide, amine and carbonyl	Cu^{2+}	4 nM	0.01-50 uM	[11]
O-phenylenediamine	carbonization	74.9: 7.8: 17.2	2.21	/	Carboxyl, amine	Cu^{2+}	145 nM	6-33 uM	[12]
Citric acid	Solvothermal method	51.5: 26.0: 22.5	0.87	41%	N-based functional groups	Cu^{2+}	40 nM	1-10 uM	[13]
L-cysteine	carbonization	63.9: 10.9: 24.10	2.21	/	Amine, hydroxyl	Cu^{2+}	47 nM	0.05-0.7/0.7-4 uM	[14]
Adenosine	Hydrothermal method	66.0: 19.0: 15.0	0.79	/	hydroxyl, amine, and carbonyl	Cu^{2+}	23 nM	0-10 uM	[15]
Iron(II) phthalocyanine	Hydrothermal method	76.6: 7.1:	2.24	/	amine	Cu^{2+}	14 nM	0.02-30 μM	[16]

15.9

Table. S2 The detection of Cu2+ in real samples.

Sample	Added Cu^{2+}(μM)	Found Cu^{2+}(μM)	Recovery(%)	RSD(n=3，%)
Tap water	10	9.54±0.17	95.4±1.7	0.97
	20	21.06±0.16	105.3±0.8	0.20
	30	29.5±0.3	98.3±1.0	0.11
Jinjiang river	10	10.62±0.14	106.2±1.4	0.16
	20	21.18±0.12	105.9±0.6	0.26
	30	28.84±0.06	96.1±0.2	0.09
Lots pond	10	10.52±0.15	105.2±1.5	0.69
	20	21.30±0.19	106.5±1.0	0.41
	30	31.82±0.14	106.1±0.4	0.19

References

1. Deng, Y.; Chen, M.; Chen, G.; Zou, W.; Zhao, Y.; Zhang, H.; Zhao, Q. Visible–Ultraviolet Upconversion Carbon Quantum Dots for Enhancement of the Photocatalytic Activity of Titanium Dioxide. *ACS Omega* **2021**, *6*, 4247-4254, doi:10.1021/acsomega.0c05182.
2. Mao, Z.; Li, H.; Gan, N.; Suo, Z.; Zhang, H.; Zhao, Q. Contribution of nicotinamide as an intracyclic N dopant to the structure and properties of carbon dots synthesized using three α-hydroxy acids as C sources. *Nanotechnology* **2022**, *33*, 215705, doi:10.1088/1361-6528/ac553e.
3. Wu, H.; Pang, L.-F.; Fu, M.-J.; Guo, X.-F.; Wang, H. Boron and nitrogen codoped carbon dots as fluorescence sensor for Fe3+ with improved selectivity. *J. Pharm. Biomed. Anal.* **2020**, *180*, 113052, doi:https://doi.org/10.1016/j.jpba.2019.113052.
4. Liu, L.; Qin, K.; Yin, S.; Zheng, X.; Li, H.; Yan, H.; Song, P.; Ji, X.; Zhang, Q.; Wei, Y.; et al. Bifunctional Carbon Dots Derived From an Anaerobic Bacterium of Porphyromonas gingivalis for Selective Detection of Fe3+ and Bioimaging. *Photochemistry and Photobiology* **2021**, *97*, 574-581, doi:https://doi.org/10.1111/php.13360.
5. Fu, Y.; Zhao, S.; Wu, S.; Huang, L.; Xu, T.; Xing, X.; Lan, M.; Song, X. A carbon dots-based fluorescent probe for turn-on sensing of ampicillin. *Dyes and Pigments* **2020**, *172*, 107846, doi:https://doi.org/10.1016/j.dyepig.2019.107846.
6. Zhang, Z.; Chen, X.; Wang, J. Bright blue emissions N-doped carbon dots from a single precursor and their application in the trace detection of Fe3+ and F^-. *Inorg. Chim. Acta* **2021**, *515*, 120087, doi:https://doi.org/10.1016/j.ica.2020.120087.

7. Zhou, Y.; Chen, G.; Ma, C.; Gu, J.; Yang, T.; Li, L.; Gao, H.; Xiong, Y.; Wu, Y.; Zhu, C.; et al. Nitrogen-doped carbon dots with bright fluorescence for highly sensitive detection of Fe3+ in environmental waters. *Spectrochim. Acta A Mol. Biomol. Spectrosc.* **2023**, 122414, doi:https://doi.org/10.1016/j.saa.2023.122414.
8. Krishnaiah, P.; Atchudan, R.; Perumal, S.; Salama, E.-S.; Lee, Y.R.; Jeon, B.-H. Utilization of waste biomass of Poa pratensis for green synthesis of n-doped carbon dots and its application in detection of Mn2+ and Fe3+. *Chemosphere* **2022**, *286*, 131764, doi:https://doi.org/10.1016/j.chemosphere.2021.131764.
9. Qian, Z.; Shan, X.; Chai, L.; Ma, J.; Chen, J.; Feng, H. Si-Doped Carbon Quantum Dots: A Facile and General Preparation Strategy, Bioimaging Application, and Multifunctional Sensor. *ACS Applied Materials & Interfaces* **2014**, *6*, 6797-6805, doi:10.1021/am500403n.
10. Gao, B.; Chen, D.; Gu, B.; Wang, T.; Wang, Z.; xie, F.; Yang, Y.; Guo, Q.; Wang, G. Facile and highly effective synthesis of nitrogen-doped graphene quantum dots as a fluorescent sensing probe for Cu2+ detection. *Curr. Appl. Phys.* **2020**, *20*, 538-544, doi:https://doi.org/10.1016/j.cap.2020.01.018.
11. Yang, L.; Zeng, J.; Quan, T.; Liu, S.; Deng, L.; Kang, X.; Xia, Z.; Gao, D. Liquid-liquid extraction and purification of oil red O derived nitrogen-doped highly photoluminescent carbon dots and their application as multi-functional sensing platform for Cu2+ and tetracycline antibiotics. *Microchem. J.* **2021**, *168*, 106391, doi:https://doi.org/10.1016/j.microc.2021.106391.
12. Yang, F.; Zhou, P.; Duan, C. Solid-phase synthesis of red dual-emissive nitrogen-doped carbon dots for the detection of Cu2+ and glutathione. *Microchem. J.* **2021**, *169*, 106534, doi:https://doi.org/10.1016/j.microc.2021.106534.
13. Praneerad, J.; Thongsai, N.; Supchocksoonthorn, P.; Kladsomboon, S.; Paoprasert, P. Multipurpose sensing applications of biocompatible radish-derived carbon dots as Cu2+ and acetic acid vapor sensors. *SPECTROCHIM. ACTA. A.* **2019**, *211*, 59-70, doi:https://doi.org/10.1016/j.saa.2018.11.049.
14. Li, Z.; Zhou, Q.; Li, S.; Liu, M.; Li, Y.; Chen, C. Carbon dots fabricated by solid-phase carbonization using p-toluidine and l-cysteine for sensitive detection of copper. *Chemosphere* **2022**, *308*, 136298, doi:https://doi.org/10.1016/j.chemosphere.2022.136298.
15. Zhang, W.J.; Liu, S.G.; Han, L.; Luo, H.Q.; Li, N.B. A ratiometric fluorescent and colorimetric dual-signal sensing platform based on N-doped carbon dots for selective and sensitive detection of copper(II) and pyrophosphate ion. *SENSOR ACTUAT B-CHEM* **2019**, *283*, 215-221, doi:https://doi.org/10.1016/j.snb.2018.12.012.
16. Zhang, L.C.; Yang, Y.M.; Liang, L.; Jiang, Y.J.; Li, C.M.; Li, Y.F.; Zhan, L.; Zou, H.Y.; Huang, C.Z. Lighting up of carbon dots for copper(ii) detection using an aggregation-induced enhanced strategy. *Analyst* **2022**, *147*, 417-422, doi:10.1039/D1AN02147H.